

Ultrafast all-optical manipulation of the charge-density wave in VTe₂Manuel Tuniz ¹, Davide Soranzio,² Davide Bidoggia ¹, Denny Puntel ¹, Wibke Bronsch,³ Steven L. Johnson,² Maria Peressi ^{1,4}, Fulvio Parmigiani,^{1,5,3} and Federico Cilento ^{3,*}¹*Dipartimento di Fisica, Università degli Studi di Trieste, 34127 Trieste, Italy*²*Institute for Quantum Electronics, Eidgenössische Technische Hochschule (ETH) Zürich, 8093 Zurich, Switzerland*³*Elettra - Sincrotrone Trieste S.C.p.A., Strada Statale 14, km 163.5, 34149 Trieste, Italy*⁴*ICSC - Italian Research Center on High Performance Computing, Big Data and Quantum Computing, 40121 Bologna, Italy*⁵*International Faculty, University of Cologne, Albertus-Magnus-Platz, 50923 Cologne, Germany*

(Received 18 May 2023; revised 17 October 2023; accepted 1 December 2023; published 21 December 2023)

The charge-density-wave (CDW) phase in the layered transition-metal dichalcogenide VTe₂ is strongly coupled to the band inversion involving vanadium and tellurium orbitals. In particular, this coupling leads to a selective disappearance of the Dirac-type states that characterize the normal phase, when the CDW phase sets in. Here, we investigate the broadband time-resolved reflectivity variations caused by collective and single-particle excitations in the CDW ground state of VTe₂. With the aid of density functional perturbation theory simulations we unveil the presence of two collective amplitude modes of the CDW ground state. By applying a double-pulse excitation scheme, we show the possibility to manipulate these modes, gaining insights into the coupling between these two collective excitations and demonstrating a more efficient way to perturb the CDW phase in VTe₂.

DOI: [10.1103/PhysRevResearch.5.043276](https://doi.org/10.1103/PhysRevResearch.5.043276)

I. INTRODUCTION

Understanding the interactions among different degrees of freedom turns out to be crucial for the description of many macroscopic quantum phenomena, such as high-temperature superconductivity, colossal magnetoresistance, or ferromagnetism [1–3]. In charge-density-wave (CDW) systems, electrons and phonons cooperatively condensate to form a new symmetry-broken phase below a transition temperature. The low-temperature phase is characterized by the coexistence of a spatial modulation of the conduction electron density and a periodic lattice distortion (PLD). The resulting CDW ground state exhibits new low-energy collective excitations, named amplitude (AM) and phase modes, which correspond to distortions and translations of the modulated charge density [4]. Due to this strong interplay between electronic and lattice degrees of freedom, CDW systems have been widely studied and lately, the possibility to manipulate their properties is receiving increasing attention [5–8]. Transition-metal dichalcogenides (TMDCs) are a well known family of layered materials that host a variety of CDWs [6,9–11]. Among these compounds VTe₂ is attracting wide interest since recent angle-resolved photoemission experiments have demonstrated the presence of a CDW phase which is strongly coupled to the band inversion involving vanadium 3*d* and tellurium 5*p* orbitals. As a consequence, the emergence of

the CDW phase leads to a selective disappearance of the topological Dirac-type states that characterize the normal phase [12]. The origin of this profound modification of the electronic band structure must be sought in the large lattice reconstruction that breaks the threefold rotational symmetry of the high-temperature phase. Indeed, in its normal phase VTe₂ has a CdI₂ structure, consisting of trigonal layers formed by edge-sharing VTe₆ octahedra [13]. Upon cooling, it undergoes a phase transition to the CDW phase at around 475 K [13,14]. The resulting CDW state exhibits a (3×1×1) superstructure characterized by double zigzag chains of vanadium atoms [shown in Fig. 1(a)]. This low-temperature phase supports additional phonon modes, as recently demonstrated by time-resolved reflectivity experiments [15], and its structural properties have been studied by means of ultrafast electron diffraction [16–18]. Thus, the control of the atomic motion of the atoms involved in the lattice reconstruction is expected to have a profound effect on the electronic modifications induced by the emergence of the CDW phase. In perspective, the manipulation of the CDW in VTe₂ might result in the possibility to control the topology of the system on ultrafast timescales.

In this paper, by means of broadband time-resolved optical spectroscopy (TR-OS), we investigated the ultrafast reflectivity (*R*) changes caused by collective and single-particle excitations in the low-temperature CDW phase of the material. Systematic temperature-dependent measurements prove the presence of two phonon modes coupled to the CDW phase. Using a double-pump excitation scheme, we show the possibility to manipulate the out-of-equilibrium response of the CDW phase by controlling the displacements of the vanadium atoms involved in the periodic lattice distortion. This approach is then used to gain additional insights into the coupling between these two collective excitations.

*federico.cilento@elettra.eu

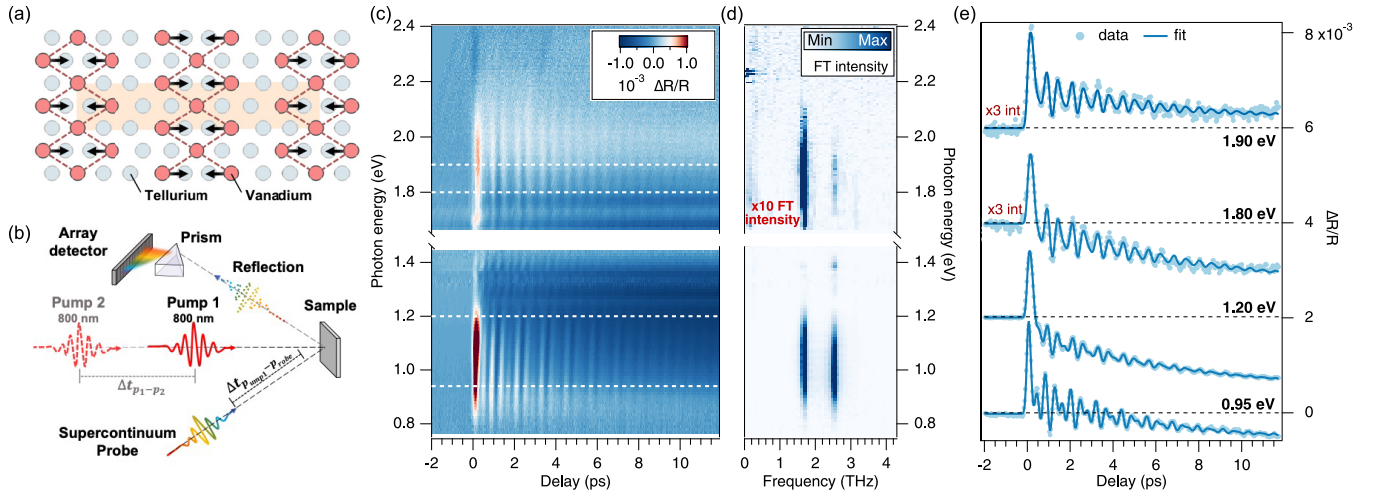


FIG. 1. (a) Top view of a VTe_2 layer in the low-temperature phase showing the lattice reconstruction that occurs in the CDW phase. The black arrows show the displacement direction of the vanadium atoms while the dashed lines highlight the shortest V-V bonds forming the double zigzag structure. The conventional unit cell is indicated by the orange rectangle behind the atoms. (b) Sketch of the time-resolved broadband reflectivity experimental setup. The reflected probe beam is dispersed through a prism and detected by an InGaAs photodiode array (PDA) detector. (c) Two-dimensional map showing the evolution of the $\Delta R/R$ signal of VTe_2 as a function of the pump-probe delay and of the probe photon energy. (d) Two-dimensional map showing the magnitude of the Fourier transform (FT) of the coherent part of the $\Delta R/R$ signal extracted from (c) as a function of the frequency and of the probe photon energy. For better visibility, in the range between 1.6 and 2.4 eV the intensity of the FT has been multiplied by a factor 10. (e) Traces extracted from (c) showing the evolution of the $\Delta R/R$ signal as a function of the pump-probe delay for four selected probe photon energies.

II. METHODS

Time-resolved reflectivity experiments [Fig. 1(b)] were performed using a Ti:sapphire femtosecond laser system, delivering, at a repetition rate of 250 kHz, ~ 50 fs light pulses at a wavelength of 800 nm (1.55 eV). A broadband (0.75–2.4 eV) supercontinuum probe beam was generated in a sapphire window, while as a pump, we used the laser fundamental at 1.55 eV. High-quality VTe_2 single crystals were obtained from HQ Graphene. Density functional theory (DFT) simulations were carried out using the QUANTUM ESPRESSO (QE) [19–21] suite of codes. Optimized norm conserving Vanderbilt pseudopotentials [22] with the generalized gradient approximation (GGA) in the Perdew-Burke-Ernzerhof (PBE) parametrization for the exchange-correlation functional [23] were employed. To confirm the results, additional calculations were performed using ultrasoft pseudopotentials (see Supplemental Material [24]). A $12 \times 12 \times 8$ Monkhorst-Pack k -point mesh was used in sampling the reciprocal space, while cutoff values of 150 and 450 Ry were respectively employed for wave-function and charge-density representations. In order to correctly reproduce the interlayer interaction, the van der Waals contribution was explicitly added by using the Grimme D2 method [25]. Starting from a monoclinic unit cell with the experimental structural parameters $a = 18.984$ Å, $b = 3.595$ Å, $c = 9.069$ Å, and $\beta = 134.62^\circ$ [13], we got the DFT optimized parameters $a = 18.928$ Å, $b = 3.577$ Å, $c = 9.148$ Å, and $\beta = 133.3^\circ$, that we used in the following calculations. To obtain the zone-center phonon eigenvalues and eigenvectors, the dynamical matrix was calculated and diagonalized in a density functional perturbation theory (DFPT) [26] approach under the scalar relativistic approximation [27] as implemented in QE.

III. RESULTS AND DISCUSSION

The two-dimensional map reported in Fig. 1(c) shows the evolution of the $\Delta R/R$ signal as a function of the pump-probe delay in the spectral range accessible through our supercontinuum probe. The measurement was performed at 80 K, at an incident fluence of ≈ 490 $\mu\text{J}/\text{cm}^2$. Therefore, considering the high critical CDW temperature of this material, we reside in the low perturbation regime. Indeed, for an incident fluence of 490 $\mu\text{J}/\text{cm}^2$, we estimated the single-pulse-induced lattice heating to be of ≈ 230 K [24]. The spectral region around 1.5 eV was disturbed by the pump photons scattered from the sample, so it was not considered. For a wide range of probe photon energies the nonequilibrium reflectivity is dominated by the presence of strong coherent oscillations which add up to the incoherent, exponentially decaying signal. As for other CDW systems, below the critical temperature, the incoherent response of the system shows a first fast decay that vanishes within 1 ps and a slow recovery process on a timescale of ~ 10 ps [28–30]. The former, which usually slows down critically upon approaching the critical temperature, is attributed to the recombination time of hot carriers across the temperature-dependent CDW gap [30], while the latter is attributed to a second stage of the CDW recovery, as detailed studies of the dynamics as a function of the excitation fluence and applied external electric field have shown in several CDW materials [3,9]. Figure 1(d) shows the square magnitude of the Fourier transform of the coherent part of the signal, isolated by subtracting a double exponential decay fit function to the data shown in Fig. 1(c). Two sharp peaks at a frequency of ~ 1.65 and ~ 2.50 THz appear over a wide range of photon energies [15]. As confirmed by our DFPT calculations, these frequencies are linked to A_1 zone-center optical phonon

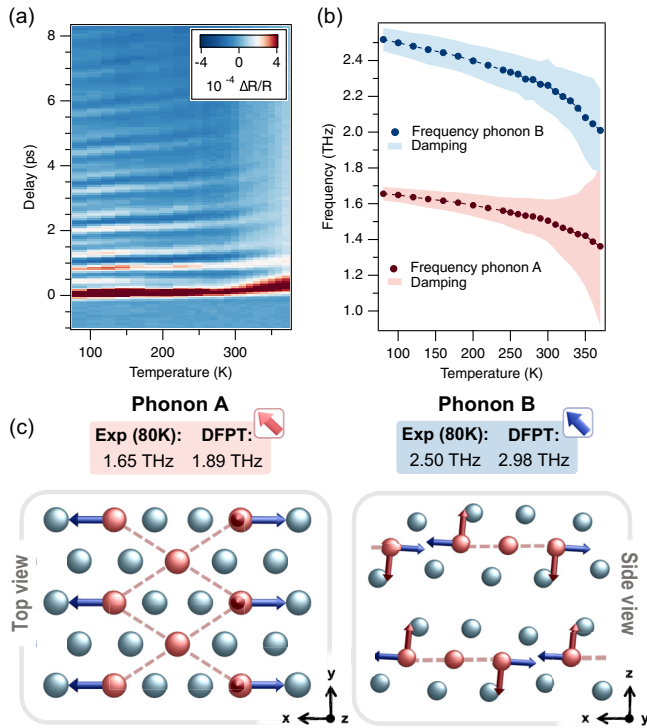


FIG. 2. (a) Two-dimensional map showing the evolution of the $\Delta R/R$ signal as a function of the temperature and of the pump-probe delay. The measurements have been performed at a probe photon energy of ~ 0.95 eV (1300 nm). (b) Evolution of the frequency and the damping (shaded areas whose widths correspond to the damping) of the two phonon modes as a function of the temperature. The renormalization of the frequency follows the behavior expected from a mean-field description. (c) Schematic representation of the displacements of the vanadium atoms associated with phonon A (red arrows) and phonon B (blue arrow). Vanadium atoms are in red, and tellurium atoms are in teal. The colored boxes show a comparison between the experimental and the calculated frequency of the two phonon modes.

modes [see the discussion for Fig. 2(c)]. For notation purposes, since their actual frequency varies with the temperature as we will show in the following, we refer to these modes labeling “A” the one with a low-temperature frequency of ~ 1.65 THz and “B” the one with a frequency of ~ 2.50 THz. With the aim of tracking the dependence of both coherent and incoherent parts of the out-of-equilibrium reflectivity on the probe photon energy, we model the full temporal evolution after the perturbation (time zero, $t = 0$) as

$$\frac{\Delta R}{R}(t, h\nu) = G(t) \otimes \left[\sum_{i=1}^2 A_i(h\nu) e^{-t/\tau_i^e(h\nu)} + B(h\nu) + \sum_{j=1}^2 C_j(h\nu) e^{-t/\tau_j^{\text{ph}}} \cos[\omega_j t + \phi_j(h\nu)] \right], \quad (1)$$

where $G(t)$ represents the cross correlation between the pump and probe pulses corresponding to the temporal resolution of our experiments, which turns out to be ≈ 150 fs. $A_i(h\nu)$ denotes the amplitude of the electronic relaxation phenomena

with time constant $\tau_i^e(h\nu)$. $B(h\nu)$ represents the amplitude of a much slower process (likely related to the heating of the sample) that in our time window can be approximated by a constant term. Finally, $C_j(h\nu)$ denotes the amplitude of the oscillation due to the excitation of coherent phonons with angular frequency ω_j , phase $\phi_j(h\nu)$, and decay time τ_j^{ph} . It is worth noting that the use of a broadband probe offers the unique possibility to study not only the relaxation dynamics of the material but also the effect of the phonon modes on the optical properties over a wide range of energies.

In Fig. 1(e) we show four traces extracted at selected photon energies from Fig. 1(c) together with the best fits obtained by using Eq. (1). For energies below 1.3 eV a strong beat between the two modes is clearly visible, while for higher energies there is a predominant contribution of phonon A. As shown in the work by Mitsuishi *et al.* [12] and confirmed by our density of states calculations [24], for energies of ~ 1 eV the probe beam is resonant with the transition between the hybridized bonding and nonbonding vanadium states above the Fermi level which are strongly affected by the emergence of the CDW phase [24]. The fact that for these energies we observe a strong enhancement in the amplitude of the oscillations constitutes evidence of the link between these phonon modes and the CDW phase.

Therefore, to study the origin of these phonon modes and, in particular, their interplay with the CDW phase, we performed a systematic study of the evolution of the nonequilibrium reflectivity as a function of the temperature. To this end we focused our attention to the infrared region of the spectrum, where the modulation of the reflectivity due to the two phonon modes is largest. Moreover, to improve the signal-to-noise ratio, we performed single-color measurements by filtering the supercontinuum probe beam with a bandpass filter at ~ 0.95 eV (1300 nm), allowing therefore to adopt a lock-in detection of a single InGaAs photodiode. The two-dimensional map in Fig. 2(a) shows the evolution of the nonequilibrium reflectivity signal as a function of the temperature while Fig. 2(b) shows the renormalization of the frequency and evolution of the damping of the two modes [24]. As shown by these two images, a strong renormalization of the frequency of the two phonon modes occurs upon increasing the temperature towards the CDW critical temperature. This effect goes along with an exponential increase of the damping [$\Gamma = 1/(\pi\tau^{\text{ph}})$] of the two modes at high temperatures. This peculiar behavior has been observed in several CDW systems and it is often considered the fingerprint of the amplitude mode of the system [29–35]. Remarkably, VTe₂ shows a rather unusual behavior with two modes strongly intertwined to the CDW phase. This observation is confirmed by our DFT simulations. Figure 2(c) shows the eigendisplacements of the two phonon modes for the vanadium atoms involved in the CDW reconstruction. For both phonon modes there is a component of the motion along the direction of the CDW reconstruction [x axis in Fig. 2(c)], meaning that the two modes can modulate the amplitude of the CDW, as expected from the amplitude mode of the system [4,36,37]. Even if both phonons are intertwined with the CDW reconstruction, as shown in Fig. 2(c), for phonon B the movement of the vanadium atoms is more localized along the direction of the PLD, therefore this mode is expected to modulate the CDW

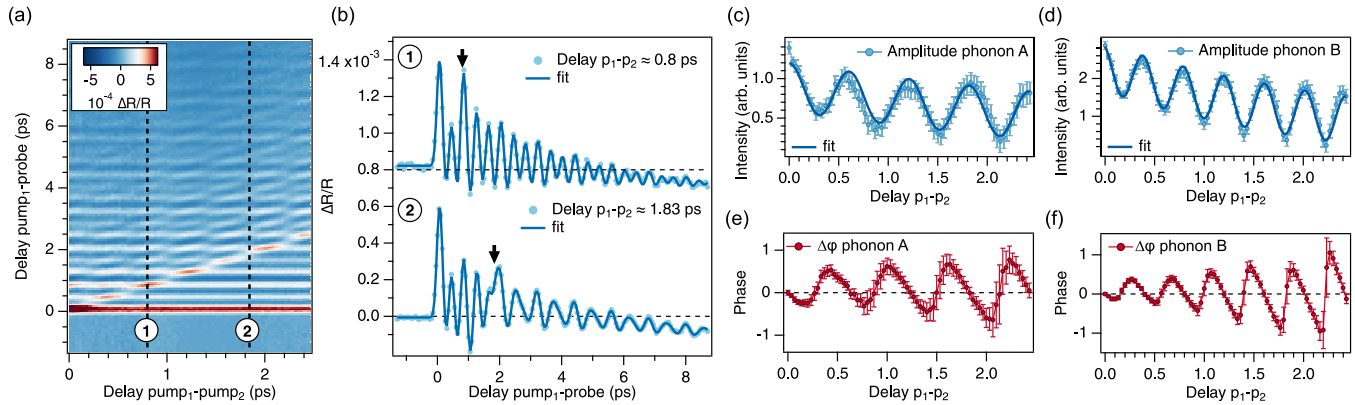


FIG. 3. (a) Two-dimensional map showing the evolution of the $\Delta R/R$ signal as a function of the delay between the two pump pulses (x axis) and the delay between the first pump and the probe pulses (y axis). The measurements have been performed at a probe photon energy of ~ 0.95 eV (1300 nm). (b) Traces extracted from (a) together with their best fits showing the evolution of the $\Delta R/R$ signal as a function of the delay between the first pump and the probe pulses for two selected delays between the pump pulses [24]. The black arrows show the arrival of the second pump pulse. (c)–(e) Evolution of the amplitude and of the phase shift of the two phonon modes as a function of the delay between the two pump pulses.

reconstruction more effectively. This observation is in agreement with the fact that this mode shows a more pronounced temperature renormalization of the frequency, meaning that it is more affected by the CDW disappearance. Conversely, phonon A involves smaller displacements along the lattice reconstruction and more pronounced out-of-plane movements of the vanadium atoms. We also note that there is reasonable agreement among the calculated and the experimental values of the frequencies, given the fact that the measurements have been performed at 80 K while the calculations have been performed in the zero-temperature limit. We expect to have a further increase of the frequencies at lower temperatures [4,38].

The observation of two amplitude modes in this material leads one to wonder whether these two are mutually coupled or whether they independently modulate the CDW order parameter. Additional insight into this coupling can be gained from double-pump experiments. In particular, coherent control of phonon modes have been demonstrated in a wide variety of crystalline materials, including conventional quasi-one-dimensional (1D) CDW systems [39–44], and can be used to study the coupling between different modes [45]. Here, we apply this approach to the case of VTe_2 , where two phonon modes are directly coupled to the CDW phase. In general, after photoexcitation, the motion of the vanadium atoms in real space is defined by the combination of the displacements given by the two phonon modes described above. Using a double-pump excitation scheme and tuning the relative delay between the pump pulses, it is possible to selectively enhance or reduce the amplitude of one of two modes and hence it is possible to partially control the atomic motion of the vanadium atoms in real space. We show the results of this approach in the two-dimensional map reported in Fig. 3(a), where the evolution of the $\Delta R/R$ signal is studied as a function of the delay between the two pump pulses. In order to better visualize the effect of the second pump pulse on the oscillations induced by the phonon modes in Fig. 3(b) we show two traces extracted from Fig. 3(a) at selected delays between the two

pump pulses. For this experiment we set the incident fluence to be $F_{p_1} = 2F_{p_2} \approx 450 \mu\text{J}/\text{cm}^2$.

Trace 1 in Fig. 3(b) shows the effect of a second excitation which is in phase with phonon B but almost completely out of phase with phonon A. The result is a strong enhancement of the amplitude of the former and a suppression of the latter. This implies that [as shown in Fig. 2(c)] the large out-of-plane component in the movement of vanadium atoms, given by the excitation of phonon A, is deeply reduced while the movement along the coordinate of the PLD is amplified, resulting in a stronger perturbation of the CDW phase. Trace 2 in Fig. 3(b) shows the opposite case. Indeed, the excitation of the second pump pulse here is in phase with phonon A but out of phase with phonon B. This leads to an enhancement of the displacements along the direction perpendicular to the CDW reconstruction. It is worth nothing that both these configurations are markedly different from the ones that can be reached using a single-pump excitation.

From the evolution of the amplitude of the two modes as a function of the delay between the two pump pulses we can gain information on the coupling between the two modes. Indeed, the fact that we can selectively control the amplitude of each mode separately, points to an independent nature of the two amplitude modes [45]. This observation is further corroborated by the fact that the complete evolution of the amplitude of the two modes shown in Figs. 3(c) and 3(d) can be described by using a model for two independent oscillators [24]. It is worth nothing that the absence of coupling between the amplitude modes in the photoexcited phase is particularly interesting, since both are coupled to the same electronic order parameter and modulate the movement of the same atoms. Finally, the double-excitation scheme allows us to control the phase of the phonon modes [24,46]. Indeed, the second pump pulse induces a phase shift in the motion of the atoms. As shown by Figs. 3(e) and 3(f), the extent of the phase shift depends on the delay between the two pump pulses. This effect originates from the fact that, since the two phonon modes are described by damped cosine oscillations, as time passes their

intensity decreases (exponentially) while the intensity of the second pump pulse remains fixed. Hence, the effect of the second pump pulse grows with the delay between the two pump pulses.

IV. CONCLUSIONS

In conclusion, our TR-OS experiments have revealed the presence of two distinct phonon modes coupled the CDW in VTe_2 . As confirmed by our DFT simulations, both modes modulate the amplitude of the lattice reconstruction, hence affecting the charge order. Using a double-pump excitation scheme we have shown the possibility to manipulate the out-of-equilibrium response of the CDW phase by selectively controlling the displacements of the vanadium atoms involved in the periodic lattice distortion. Moreover, this approach has allowed us to study the coupling between the two amplitude modes, showing that the two are decoupled in the photoex-

cited state. Our finding of a more efficient way to perturb the CDW in VTe_2 constitutes a crucial step towards the possibility to control the topology of the electronic structure on ultrafast timescales.

ACKNOWLEDGMENTS

This work was partially supported by the Swiss National Science Foundation under Project No. 200020_192337. Computational resources have been obtained from CINECA through the ISCRA initiative and the agreement with the University of Trieste. M.P. acknowledges support from Fondazione ICSC - “Italian Research Center on High-Performance Computing, Big Data and Quantum Computing” - Spoke 7, Materials and Molecular Sciences - National Recovery and Resilience Plan (PNRR) - funded by MUR Missione 4 - Componente 2 - Investimento 1.4 - Next Generation EU (NGEU).

-
- [1] Y. Tokura, M. Kawasaki, and N. Nagaosa, Emergent functions of quantum materials, *Nat. Phys.* **13**, 1056 (2017).
- [2] D. N. Basov, R. D. Averitt, and D. Hsieh, Towards properties on demand in quantum materials, *Nat. Mater.* **16**, 1077 (2017).
- [3] M. Eichberger, H. Schäfer, M. Krumova, M. Beyer, J. Demsar, H. Berger, G. Moriena, G. Sciaini, and R. J. D. Miller, Snapshots of cooperative atomic motions in the optical suppression of charge density waves, *Nature (London)* **468**, 799 (2010).
- [4] G. Grüner, *Density Waves in Solids* (Addison-Wesley, Reading, MA, 1994).
- [5] S. Duan, Y. Cheng, W. Xia, Y. Yang, C. Xu, F. Qi, C. Huang, T. Tang, Y. Guo, W. Luo, D. Qian, D. Xiang, J. Zhang, and W. Zhang, Optical manipulation of electronic dimensionality in a quantum material, *Nature (London)* **595**, 239 (2021).
- [6] L. Stojchevska, I. Vaskivskiy, T. Mertelj, P. Kusar, D. Svetin, S. Brazovskii, and D. Mihailovic, Ultrafast switching to a stable hidden quantum state in an electronic crystal, *Science* **344**, 177 (2014).
- [7] A. Zong, X. Shen, A. Kogar, L. Ye, C. Marks, D. Chowdhury, T. Rohwer, B. Freelon, S. Weathersby, R. Li, J. Yang, J. Checkelsky, X. Wang, and N. Gedik, Ultrafast manipulation of mirror domain walls in a charge density wave, *Sci. Adv.* **4**, eaau5501 (2018).
- [8] J. Maklar, Y. W. Windsor, C. W. Nicholson, M. Puppini, P. Walmsley, V. Esposito, M. Porer, J. Rittmann, D. Leuenberger, M. Kubli, M. Savoini, E. Abreu, S. L. Johnson, P. Beaud, G. Ingold, U. Staub, I. R. Fisher, R. Ernstorfer, M. Wolf, and L. Rettig, Nonequilibrium charge-density-wave order beyond the thermal limit, *Nat. Commun.* **12**, 2499 (2021).
- [9] G. Storeck, J. G. Horstmann, T. Diekmann, S. Vogelgesang, G. von Witte, S. V. Yalunin, K. Rossnagel, and C. Ropers, Structural dynamics of incommensurate charge-density waves tracked by ultrafast low-energy electron diffraction, *Struct. Dyn.* **7**, 034304 (2020).
- [10] T. Huber, S. O. Mariager, A. Ferrer, H. Schäfer, J. A. Johnson, S. Grübel, A. Lübcke, L. Huber, T. Kubacka, C. Dornes, C. Laulhe, S. Ravy, G. Ingold, P. Beaud, J. Demsar, and S. L. Johnson, Coherent structural dynamics of a prototypical charge-density-wave-to-metal transition, *Phys. Rev. Lett.* **113**, 026401 (2014).
- [11] M. Porer, U. Leierseder, J.-M. Ménard, H. Dachraoui, L. Mouchliadis, I. E. Perakis, U. Heinzmann, J. Demsar, K. Rossnagel, and R. Huber, Non-thermal separation of electronic and structural orders in a persisting charge density wave, *Nat. Mater.* **13**, 857 (2014).
- [12] N. Mitsuishi, Y. Sugita, M. S. Bahramy, M. Kamitani, T. Sonobe, M. Sakano, T. Shimojima, H. Takahashi, H. Sakai, K. Horiba, H. Kumigashira, K. Taguchi, K. Miyamoto, T. Okuda, S. Ishiwata, Y. Motome, and K. Ishizaka, Switching of band inversion and topological surface states by charge density wave, *Nat. Commun.* **11**, 2466 (2020).
- [13] K. Bronsema, G. Bus, and G. Wiegers, The crystal structure of vanadium ditelluride, $V_{1+x}Te_2$, *J. Solid State Chem.* **53**, 415 (1984).
- [14] T. Ohtani, K. Hayashi, M. Nakahira, and H. Nozaki, Phase transition in $V_{1+x}Te_2$ ($0.04 \leq x \leq 0.11$), *Solid State Commun.* **40**, 629 (1981).
- [15] H. Tanimura, N. L. Okamoto, T. Homma, Y. Sato, A. Ishii, H. Takamura, and T. Ichitsubo, Nonthermal melting of charge density wave order via nucleation in VTe_2 , *Phys. Rev. B* **105**, 245402 (2022).
- [16] A. Nakamura, T. Shimojima, M. Matsuura, Y. Chiashi, M. Kamitani, H. Sakai, S. Ishiwata, H. Li, A. Oshiyama, and K. Ishizaka, Evaluation of photo-induced shear strain in monoclinic VTe_2 by ultrafast electron diffraction, *Appl. Phys. Express* **11**, 092601 (2018).
- [17] A. Nakamura, T. Shimojima, Y. Chiashi, M. Kamitani, H. Sakai, S. Ishiwata, H. Li, and K. Ishizaka, Nanoscale imaging of unusual photoacoustic waves in thin flake VTe_2 , *Nano Lett.* **20**, 4932 (2020).
- [18] T. Suzuki, Y. Kubota, N. Mitsuishi, S. Akatsuka, J. Koga, M. Sakano, S. Masubuchi, Y. Tanaka, T. Togashi, H. Ohsumi, K. Tamasaku, M. Yabashi, H. Takahashi, S. Ishiwata, T. Machida, I. Matsuda, K. Ishizaka, and K. Okazaki, Ultrafast control of the crystal structure in a topological charge-density-wave material, *Phys. Rev. B* **108**, 184305 (2023).

- [19] P. Giannozzi, S. Baroni, N. Bonini, M. Calandra, R. Car, C. Cavazzoni, D. Ceresoli, G. L. Chiarotti, M. Cococcioni, I. Dabo, A. Dal Corso, S. de Gironcoli, S. Fabris, G. Fratesi, R. Gebauer, U. Gerstmann, C. Gougoussis, A. Kokalj, M. Lazzeri, L. Martin-Samos *et al.*, QUANTUM ESPRESSO: A modular and open-source software project for quantum simulations of materials, *J. Phys.: Condens. Matter* **21**, 395502 (2009).
- [20] P. Giannozzi, O. Andreussi, T. Brumme, O. Bunau, M. B. Nardelli, M. Calandra, R. Car, C. Cavazzoni, D. Ceresoli, M. Cococcioni, N. Colonna, I. Carnimeo, A. D. Corso, S. de Gironcoli, P. Delugas, R. A. DiStasio Jr, A. Ferretti, A. Floris, G. Fratesi, G. Fugallo *et al.*, Advanced capabilities for materials modelling with QUANTUM ESPRESSO, *J. Phys.: Condens. Matter* **29**, 465901 (2017).
- [21] P. Giannozzi, O. Baseggio, P. Bonfà, D. Brunato, R. Car, I. Carnimeo, C. Cavazzoni, S. de Gironcoli, P. Delugas, F. F. Ruffino, A. Ferretti, N. Marzari, I. Timrov, A. Urru, and S. Baroni, QUANTUM ESPRESSO toward the exascale, *J. Chem. Phys.* **152**, 154105 (2020).
- [22] D. R. Hamann, Optimized norm-conserving Vanderbilt pseudopotentials, *Phys. Rev. B* **88**, 085117 (2013).
- [23] J. P. Perdew, J. A. Chevary, S. H. Vosko, K. A. Jackson, M. R. Pederson, D. J. Singh, and C. Fiolhais, Atoms, molecules, solids, and surfaces: Applications of the generalized gradient approximation for exchange and correlation, *Phys. Rev. B* **46**, 6671 (1992).
- [24] See Supplemental Material at <http://link.aps.org/supplemental/10.1103/PhysRevResearch.5.043276> for complementary data and detailed information on the fitting procedure.
- [25] S. Grimme, Density functional theory with London dispersion corrections, *WIREs Comput. Mol. Sci.* **1**, 211 (2011).
- [26] S. Baroni, S. de Gironcoli, A. Dal Corso, and P. Giannozzi, Phonons and related crystal properties from density-functional perturbation theory, *Rev. Mod. Phys.* **73**, 515 (2001).
- [27] T. Takeda, The scalar relativistic approximation, *Z. Phys. B* **32**, 43 (1978).
- [28] H. Schaefer, M. Koerber, A. Tomelj, K. Biljaković, H. Berger, and J. Demsar, Dynamics of charge density wave order in the quasi one dimensional conductor $(\text{TaSe}_4)_2\text{I}$ probed by femtosecond optical spectroscopy, *Eur. Phys. J.: Spec. Top.* **222**, 1005 (2013).
- [29] H. Schäfer, V. V. Kabanov, M. Beyer, K. Biljakovic, and J. Demsar, Disentanglement of the electronic and lattice parts of the order parameter in a 1D charge density wave system probed by femtosecond spectroscopy, *Phys. Rev. Lett.* **105**, 066402 (2010).
- [30] J. Demsar, K. Biljaković, and D. Mihailovic, Single particle and collective excitations in the one-dimensional charge density wave solid $\text{K}_{0.3}\text{MoO}_3$ probed in real time by femtosecond spectroscopy, *Phys. Rev. Lett.* **83**, 800 (1999).
- [31] N. Yoshikawa, H. Sugauma, H. Matsuoka, Y. Tanaka, P. Hemme, M. Cazayous, Y. Gallais, M. Nakano, Y. Iwasa, and R. Shimano, Ultrafast switching to an insulating-like metastable state by amplitudon excitation of a charge density wave, *Nat. Phys.* **17**, 909 (2021).
- [32] R. Y. Chen, S. J. Zhang, M. Y. Zhang, T. Dong, and N. L. Wang, Revealing extremely low energy amplitude modes in the charge-density-wave compound LaAgSb_2 , *Phys. Rev. Lett.* **118**, 107402 (2017).
- [33] R. V. Yusupov, T. Mertelj, J.-H. Chu, I. R. Fisher, and D. Mihailovic, Single-particle and collective mode couplings associated with 1- and 2-directional electronic ordering in metallic $R\text{Te}_3$ ($R = \text{Ho, Dy, Tb}$), *Phys. Rev. Lett.* **101**, 246402 (2008).
- [34] C. N. Kuo, D. Shen, B. S. Li, N. N. Quyen, W. Y. Tzeng, C. W. Luo, L. M. Wang, Y. K. Kuo, and C. S. Lue, Characterization of the charge density wave transition and observation of the amplitude mode in LaAuSb_2 , *Phys. Rev. B* **99**, 235121 (2019).
- [35] A. Tomelj, H. Schäfer, D. Städter, M. Beyer, K. Biljakovic, and J. Demsar, Dynamics of photoinduced charge-density-wave to metal phase transition in $\text{K}_{0.3}\text{MoO}_3$, *Phys. Rev. Lett.* **102**, 066404 (2009).
- [36] S. Hellmann, T. Rohwer, M. Kalläne, K. Hanff, C. Sohr, A. Stange, A. Carr, M. M. Murnane, H. C. Kapteyn, L. Kipp, M. Bauer, and K. Rossnagel, Time-domain classification of charge-density-wave insulators, *Nat. Commun.* **3**, 1069 (2012).
- [37] C. Sohr, A. Stange, M. Bauer, and K. Rossnagel, How fast can a Peierls-Mott insulator be melted?, *Faraday Discuss.* **171**, 243 (2014).
- [38] H. Schaefer, V. V. Kabanov, and J. Demsar, Collective modes in quasi-one-dimensional charge-density wave systems probed by femtosecond time-resolved optical studies, *Phys. Rev. B* **89**, 045106 (2014).
- [39] D. Mihailovic, D. Dvorsek, V. V. Kabanov, J. Demsar, L. Forró, and H. Berger, Femtosecond data storage, processing, and search using collective excitations of a macroscopic quantum state, *Appl. Phys. Lett.* **80**, 871 (2002).
- [40] O. Y. Gorobtsov, L. Ponet, S. K. K. Patel, N. Hua, A. G. Shabalin, S. Hrkac, J. Wingert, D. Cela, J. M. Glowina, D. Zhu, R. Medapalli, M. Chollet, E. E. Fullerton, S. Artyukhin, O. G. Shpyrko, and A. Singer, Femtosecond control of phonon dynamics near a magnetic order critical point, *Nat. Commun.* **12**, 2865 (2021).
- [41] M. J. Neugebauer, T. Huber, M. Savoini, E. Abreu, V. Esposito, M. Kubli, L. Rettig, E. Bothschafter, S. Grübel, T. Kubacka, J. Rittmann, G. Ingold, P. Beaud, D. Dominko, J. Demsar, and S. L. Johnson, Optical control of vibrational coherence triggered by an ultrafast phase transition, *Phys. Rev. B* **99**, 220302(R) (2019).
- [42] S. Michael and H. C. Schneider, Optical amplification in a charge density wave phase of a quasi-two-dimensional material, *Phys. Rev. B* **105**, 235108 (2022).
- [43] K. G. Nakamura, K. Yokota, Y. Okuda, R. Kase, T. Kitashima, Y. Mishima, Y. Shikano, and Y. Kayanuma, Ultrafast quantum-path interferometry revealing the generation process of coherent phonons, *Phys. Rev. B* **99**, 180301(R) (2019).
- [44] A. Bartels, T. Dekorsy, H. Kurz, and K. Köhler, Coherent control of acoustic phonons in semiconductor superlattices, *Appl. Phys. Lett.* **72**, 2844 (1998).
- [45] L. Rettig, J.-H. Chu, I. R. Fisher, U. Bovensiepen, and M. Wolf, Coherent dynamics of the charge density wave gap in tritellurides, *Faraday Discuss.* **171**, 299 (2014).
- [46] H. Sasaki, R. Tanaka, Y. Okano, F. Minami, Y. Kayanuma, Y. Shikano, and K. G. Nakamura, Coherent control theory and experiment of optical phonons in diamond, *Sci. Rep.* **8**, 9609 (2018).